Dynamical inhomogeneity of liquid Te near the melting temperature proved by inelastic x-ray scattering measurements

2008 J. Phys.: Condens. Matter 20 494244

(http://iopscience.iop.org/0953-8984/20/49/494244)

J. Phys.: Condens. Matter **20** (2008) 494244 (7pp) doi:10.1088/0953-8984/20/49/494244

Dynamical inhomogeneity of liquid Te near the melting temperature proved by inelastic x-ray scattering measurements

Y Kajihara[1], M Inui[1], S Hosokawa[2], K Matsuda[3] and A Q R Baron[4]

[1] Graduate School of Integrated Arts and Sciences, Hiroshima University, Higashi-Hiroshima 739-8521, Japan
[2] Center for Materials Research using Third-Generation Synchrotron Radiation Facilities, Hiroshima Institute of Technology, Hiroshima 731-5193, Japan
[3] Graduate School of Engineering, Kyoto University, Kyoto 606-8501, Japan
[4] SPring-8/RIKEN, 1-1-1 Kouto, Sayo-cho, Sayo-gun, Hyogo 679-5148, Japan

E-mail: kajihara@hiroshima-u.ac.jp

Received 31 July 2008, in final form 3 October 2008
Published 12 November 2008
Online at stacks.iop.org/JPhysCM/20/494244

Abstract

The high frequency dynamics of liquid Te near the melting temperature has been investigated by means of inelastic x-ray scattering measurements. Dynamic structure factors $S(Q, E)$ are obtained at 500, 650 and 800 °C. Acoustic excitation is ascertained at each temperature: its Q-dependent phase velocity $v(Q)$ switches from the high frequency value v_{IXS} to the ultrasonic value v_{s} at a certain momentum transfer ($Q = Q_{\mathrm{trans}}$). With decreasing temperature, both the 'positiveness' ($\equiv(v_{\mathrm{IXS}} - v_{\mathrm{s}})/v_{\mathrm{s}}$) and the effective length ($\equiv 2\pi/Q_{\mathrm{trans}}$) increase, which means that the structural relaxation in liquid Te changes greatly in this temperature region. With the aid of a thermodynamic formulation, we show that this should be seen as evidence of *dynamical* inhomogeneity: it can be greatly enhanced by the metal–nonmetal transition which occurs in the supercooled region. The *dynamical* inhomogeneity may be induced by a *second* critical phenomenon, which is similar to the case for liquid water.

(Some figures in this article are in colour only in the electronic version)

1. Introduction

Liquid Te has been known to be a very mysterious material and has been fascinating many researchers for over half a century. Te is a typical semiconductor in the solid phase, but it shows metallic nature in the liquid phase [1]. This change in electrical property is believed to be closely related to the structural change in Te [2]. In the solid phase, Te consists of twofold-coordinated covalently bonded chains, and a stable crystal under ambient conditions has a trigonal form which is commonly seen for solid selenium, also a chalcogen element. But on melting, the coordination number in liquid Te becomes around 3 [3], and the density becomes slightly higher than that in the solid phase. The most remarkable features of liquid Te are thermodynamic anomalies. The temperature dependence of the density shows a maximum [4] at around the melting temperature ($T_{\mathrm{m}} \simeq 450$ °C) and with increasing temperature, the heat capacity *decreases* [5] and the ultrasonic sound velocity *increases* [6, 7] near the melting temperature. These features are anomalous as compared to the behavior of normal liquids; however, they are very similar to those seen for liquid water [8] and liquid Si, which are sometimes called *anomalous liquids*. Water exhibits a density maximum at 277 K and the sound velocity of water *increases* with increasing temperature around the melting temperature.

In order to explain the thermodynamic anomalies in liquid Te, Tsuchiya and Seymour proposed an inhomogeneous structure model over twenty years ago [9]. They assumed that there exists inhomogeneity which consists of metallic and nonmetallic mesoscopic domains in liquid Te. This inhomogeneous structure model was consistent with the previous two-species model [10, 11] and inhomogeneous *transport* model [12] which had been introduced to account for the *electronic* properties (electrical conductivity, Hall

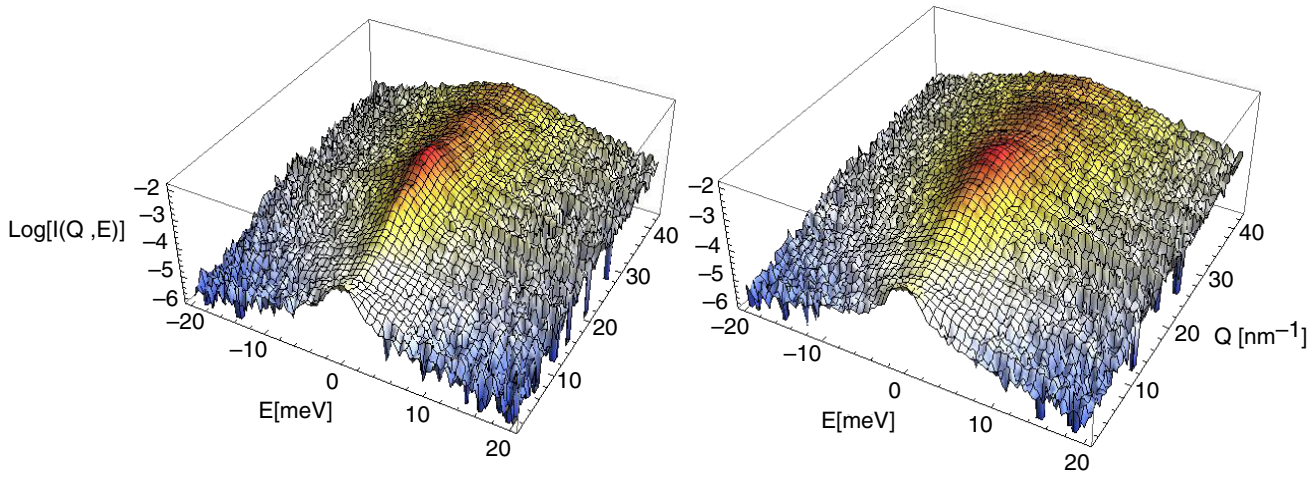

Figure 1. IXS spectra $I(Q, E)$ at 500 (left) and 800 °C (right).

coefficient and nuclear magnetic resonance Knight shift) of liquid Te. The inhomogeneous structure model partially explained both the thermodynamic anomalies and the electronic properties reasonably well, but there seem to remain two unsolved problems. The first one is that nobody has succeeded in directly observing this inhomogeneity. We know that some researchers tried to conduct small angle x-ray and neutron scattering measurements, but they observed almost no scattering intensities, resulting in no report of them. The second problem is that the model did not explain why there is inhomogeneity in liquid Te. In the model, the inhomogeneity may have been introduced only as a phenomenological input parameter.

Because of these two unsolved problems, the inhomogeneous structure model has not been widely accepted and liquid Te remains an *anomalous liquid*. In order to tackle this anomalous liquid Te, we have carried out inelastic x-ray scattering (IXS) measurements at SPring-8 in Japan. As already mentioned, liquid Te has been fascinating many researchers and up-to-date results on the local structure in liquid Te have been reported [13]. As regards the dynamical structure of liquid Te, quasi-elastic and inelastic neutron scattering (INS) measurements have been carried out to investigate the temperature dependence of the diffusive character and the vibrational density of states [14–16]. Recently studies of the dispersion of the acoustic mode at low Q were reported, involving INS [17] and IXS [18] measurements for liquid Te. However these measurements did not clarify the temperature dependence of the dispersion relation. In the previous paper [19], we reported the precise temperature dependence of the dispersion relation for the acoustic mode in liquid Te. In this paper, we report details of the experimental results and propose a concept for explaining not only IXS results but also the unsolved problems mentioned above.

2. Experiment

The experiments were carried out at the high resolution inelastic scattering beamline BL35XU of SPring-8 in Japan [20]. The energy of incident x-rays is highly monochromatized to 21.748 keV by an Si(11 11 11) back scattering monochromator, the scattered x-rays were analyzed by 12 Si crystal analyzers and the final energy resolution of the measurements was 1.5–1.8 meV HWHM.

The liquid Te sample, with a thickness of 290 μm, was contained in a thin walled single-crystalline sapphire cell [21]. The cell was located in a vessel [22] equipped with single-crystal Si windows capable of covering scattering angles between 0° and 25°. The vessel was filled with about 2 bar He gas of 99.9999% purity in order to reduce the evaporation of the liquid Te. The IXS spectra were measured and the momentum transfer ranges were between 1.3 and 43 nm^{-1} at 500 and 800 °C and between 1.3 and 27 nm^{-1} at 650 °C. Empty cell and polymethylmethacrylate (PMMA) measurements were separately carried out for background corrections and resolution function determination, respectively.

3. Results

Figure 1 shows the measured IXS spectra $I(Q, E)$ at 500 and 800 °C. The background scattering intensity from the cell is subtracted and the spectra are modified with the Q dependence of the atomic form factor. $I(Q, E = 0)$ at both temperatures shows peaks at around $Q = 20$ and 32 nm^{-1} where the static structure factors $S(Q)$ (see figure 2) exhibit maxima. With increasing temperature, these peaks become broader in both Q and E directions because the randomness of the atomic position becomes larger in both space and time. We evaluate the reliability of the present data by comparing $I(Q)$, obtained by integration of $I(Q, E)$ with respect to E as in equation (1), with $S(Q)$:

$$I(Q) = \int I(Q, E)\,\mathrm{d}E. \tag{1}$$

In figure 2(a), open circles indicate $I(Q)$ at 500 °C. It almost coincides with $S(Q)$ denoted by a solid curve, which is obtained from neutron diffraction measurements [23]. In figure 2(b), open symbols indicate $I(Q)$ in the small Q region at all temperatures. Closed symbols show $S(0)$ calculated from

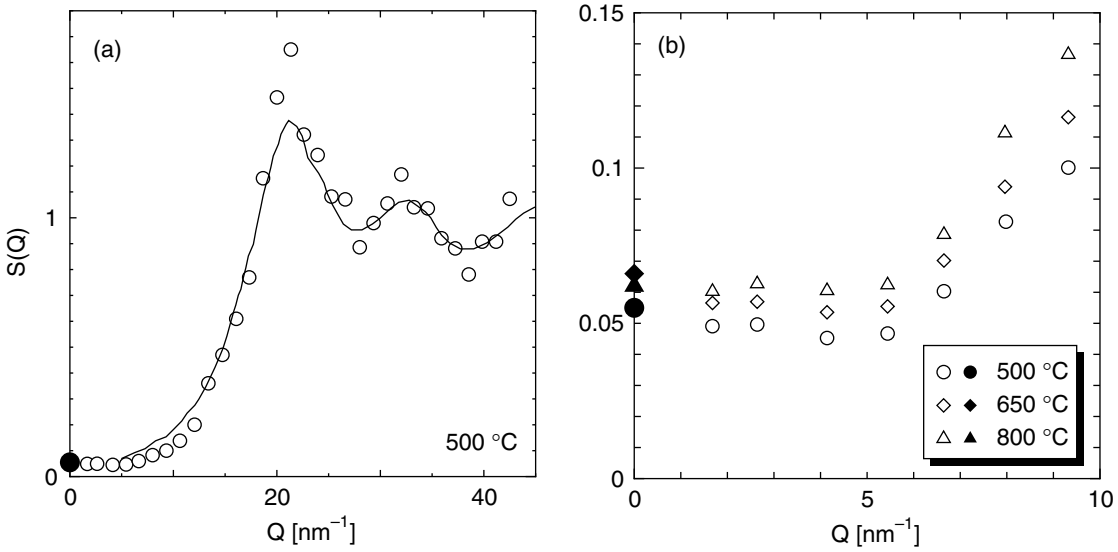

Figure 2. Static structure factors obtained from various methods (a) over the full Q region at around 500 °C and (b) for the small Q region at the temperatures in the figure. Open symbols indicate $I(Q)$ which is obtained by the integration of the present IXS spectra $I(Q, E)$ with respect to E. The solid curve and closed symbols are $S(Q)$ from ND [23] at 490 °C and the density measurements [24]. Circles, squares and triangles correspond to the data at 500, 650 and 800 °C, respectively.

the pressure (P) variation of the density (ρ) [24] using the following equation:

$$S(0) = \frac{\rho}{m} k_{\mathrm{B}} T \left[\frac{1}{\rho} \left(\frac{\partial \rho}{\partial P} \right)_T \right], \tag{2}$$

where k_{B} is the Boltzmann constant, m is the atomic mass of Te and T is the temperature. The consistency of $I(Q)$ from the present IXS and $S(0)$ from the density measurements is very good at all temperatures. There is no divergence in the small Q regions, which is consistent with the previous unpublished studies on small angle scattering, and it can be concluded that there is only a small *density* inhomogeneity in liquid Te at these temperatures.

There seem to be no distinct side peaks ($E \neq 0$) or modes in the $I(Q, E)$ spectra in figure 1, but we can certainly ascertain the acoustic mode when we analyze the spectra using a damped harmonic oscillator (DHO) model. In this model, the quasi-elastic line of a simple Lorentzian is assumed, and the inelastic mode is expressed by the DHO given as

$$\begin{aligned} \frac{I(Q,E)}{I(Q)} &= \int \frac{S(Q,E)}{S(Q)} R(R, E - E')\, \mathrm{d}E' \\ \left(\frac{S(Q,E)}{S(Q)} \right) &= \left(\frac{E/k_{\mathrm{B}}T}{1 - \mathrm{e}^{-E/k_{\mathrm{B}}T}} \right) \left[\frac{A_{\mathrm{L}}}{\pi \Gamma_{\mathrm{L}}} \frac{\Gamma_{\mathrm{L}}}{E^2 + \Gamma_{\mathrm{L}}^2} \right. \\ &\left. + \frac{A_{\mathrm{DHO}}}{\pi \hbar / k_{\mathrm{B}} T} \frac{4 \Gamma_{\mathrm{DHO}} \sqrt{E_{\mathrm{DHO}}^2 - \Gamma_{\mathrm{DHO}}^2}}{(E^2 - E_{\mathrm{DHO}}^2)^2 + 4 \Gamma_{\mathrm{DHO}}^2 E^2} \right]. \end{aligned} \tag{3}$$

Here A_{L} and Γ_{L} are the amplitude and the width of the central Lorentzian and A_{DHO}, Γ_{DHO} and E_{DHO} are the amplitude, width and energy of the DHO, respectively. $R(E)$ represents the resolution function deduced from the PMMA measurements. The parameters in the above model were optimized by the non-linear least squares method. The most important parameter in this model is $E_{\mathrm{DHO}}(Q)$ or the dispersion curve of the acoustic mode, which is indicated by open circles in figure 3 for (a) 500, (b) 650 and (c) 800 °C. The dispersal is almost linear in the small Q region, which means that we have acoustic modes, but the dispersion is much faster than that of the ultrasonic sound indicated by the dashed lines. Dips are shown at around $Q = 20$ and 32 nm^{-1} where the $S(Q)$ have maxima or pseudo-zone boundaries. These features prove that the modes are exactly the phonon-like modes. In the high Q region, they approach the dotted lines which are calculated from the thermal velocities $v_{\mathrm{th}} = \sqrt{3k_{\mathrm{B}}T/2m}$, which means that the modes represent only self-correlations in these high Q regions.

We deduce the phase velocity of the phonon-like mode by $v(Q) \equiv E_{\mathrm{DHO}}(Q)/Q$ and show the value in the small Q region using open circles in figure 4 at (a) 500, (b) 650 and (c) 800 °C. We define v_{IXS} as the $v(Q)$ value in the flat region and the *positiveness* as the normalized difference between v_{IXS} and v_{s}, $(v_{\mathrm{IXS}} - v_{\mathrm{s}})/v_{\mathrm{s}}$. This positiveness changes greatly against the temperature: from the higher temperature side, it is about 20% at 800 °C, which is a normal value for ordinary liquids. It increases with decreasing temperature, and reaches about 70% at 500 °C, which is very large compared to those for ordinary liquids. We also define Q_{trans} where $v(Q)$ approaches v_{s} in the smaller Q region (hatched area). Q_{trans} is about 2.5 nm^{-1} at 800 °C, shifts to smaller values with decreasing temperature and seems to become smaller than the smallest Q (1.5 nm^{-1}) in the present measurement at 500 °C.

Temperature dependences of these parameters are plotted in figure 5. The M–NM transition is believed to exist in the supercooled region and its transition temperature can be estimated to be around 300–350 °C [25, 26]. Sound velocities deduced by other authors are also plotted: open symbols denote the dynamical sound velocities obtained from the present IXS (circles), the previous IXS (triangles) [18]

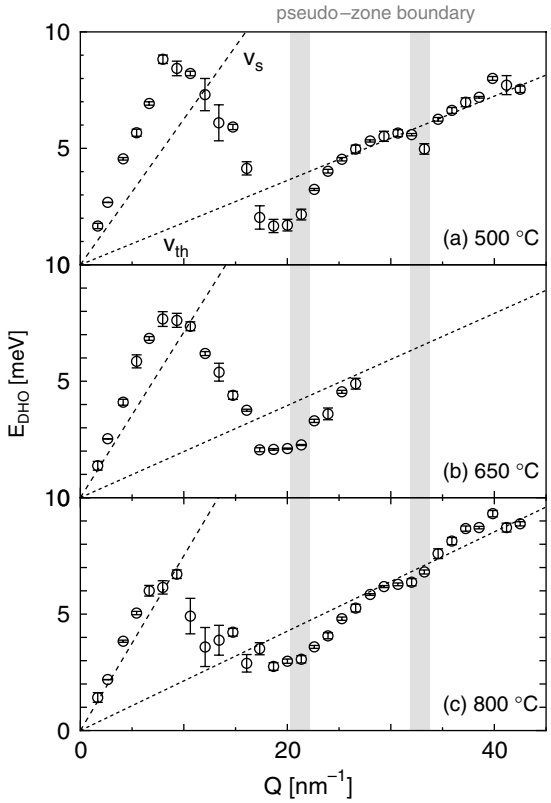

Figure 3. Dispersion curves at (a) 500, (b) 650 and (c) 800 °C. Open circles are from the present IXS experiments, and dashed lines and dotted lines are the ones from the ultrasonic sound velocities [7] and thermal velocities of atoms.

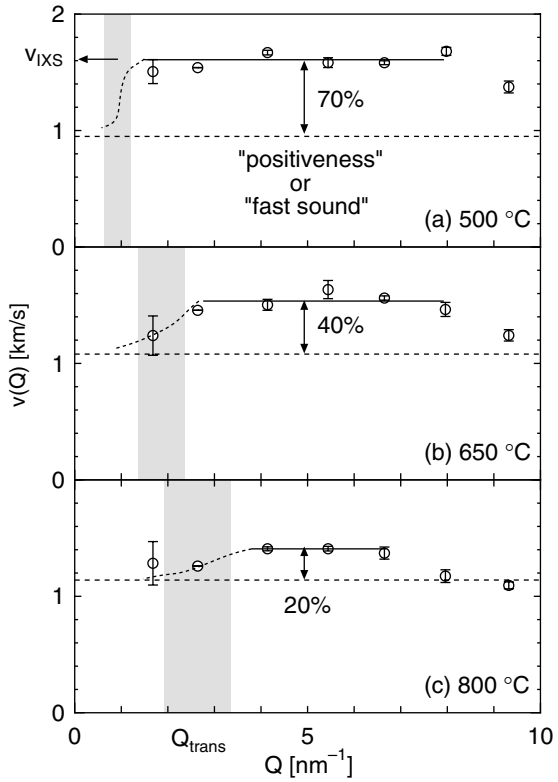

Figure 4. Open circles indicate the dependences on Q of the phase velocity $v(Q)$ at (a) 500, (b) 650 and (c) 800 °C. $v(Q)$ changes from the high frequency value v_{IXS} to the ultrasonic one v_{s} in the Q_{trans} region (hatched area). We define the *positiveness* as the normalized difference between v_{IXS} and v_{s}.

and the inelastic neutron scattering (INS; crosses) [17]. The consistency among these dynamical velocities is good. The dashed line shows the adiabatic value measured directly from the ultrasonic method [7]. With decreasing temperature, v_{IXS} normally *increases* while v_{s} anomalously *decreases*. Thus, the positiveness substantially increases with decreasing temperature. The effective length, which is defined using Q_{trans}, by $l_{\mathrm{eff}} \equiv 2\pi/Q_{\mathrm{trans}}$, and denoted by closed circles, also increases at mesoscopic order (∼nm) with decreasing temperature. The present results hint that there is a mesoscopic structural relaxation and it may be direct evidence of the *dynamical* inhomogeneity in liquid Te. In the next section, we will describe our interpretation and show what the *dynamical* inhomogeneity is and its relation with the M–NM transition.

4. Discussion

The Q dependence of the dynamical sound velocity shown in figure 4 may be regarded as the hydrodynamic viscoelastic transition commonly observed in many liquids. However, there are opposite temperature dependences of the IXS and ultrasonic sound velocities; let us consider this more carefully. The present observations clearly show that the anomalous slowing down of the ultrasonic sound with decreasing temperature is related not to the structural relaxation in the frequency region probed by the present IXS but to a much slower one. Now we discuss this from the viewpoint of thermodynamics. In fluid systems, the sound velocity v_{s} is related to the adiabatic compressibility β_S,

$$\frac{1}{\rho v_{\mathrm{s}}^2} = \beta_S = -\frac{1}{V}\left(\frac{\partial V}{\partial P}\right)_S, \tag{4}$$

where V is the molar volume of the sample and S is the entropy of the system. When the system has an internal degree of freedom x, which generates inhomogeneity, this equation should be modified to

$$\frac{1}{\rho v_{\mathrm{s}}^2} = -\frac{1}{V}\left(\frac{\partial V}{\partial P}\right)_{S,x} - \frac{1}{V}\left(\frac{\partial V}{\partial x}\right)_P \left(\frac{\partial x}{\partial P}\right)_S. \tag{5}$$

Then the excess compressibility $\beta_r \equiv -\frac{1}{V}(\frac{\partial V}{\partial x})_P(\frac{\partial x}{\partial P})_S > 0$ arises and it slows v_{s} down. When this inhomogeneity has a *dynamical* nature, which means that the inhomogeneity fluctuates with its characteristic time constant, the situation is slightly changed. In this case, if the frequency of the sound wave is high enough compared to the characteristic frequency of the fluctuations, the high frequency compressibility $\beta_{\mathrm{HF}} \equiv -\frac{1}{V}(\frac{\partial V}{\partial P})_{S,x} > 0$ is observed. These equations are established in the theory of acoustic properties [27], and here we are extending this formulation to the present IXS region. We assume that IXS gives a measure of this high frequency

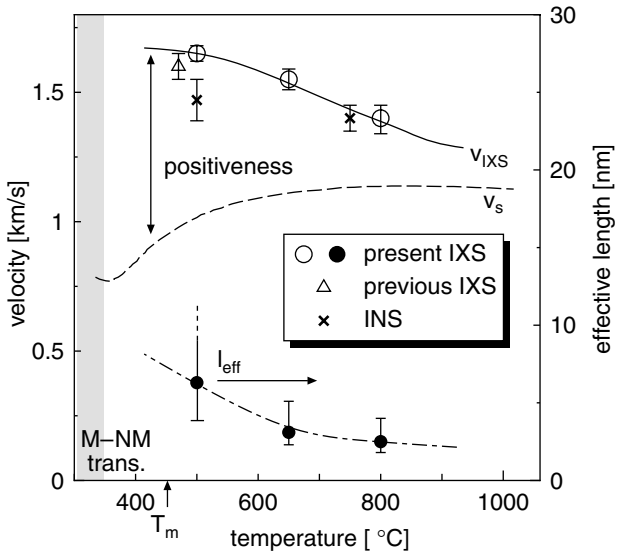

Figure 5. Sound velocities obtained from various methods and the effective length defined from the present IXS. Open symbols show the dynamical values deduced from $S(Q, E)$ for the present IXS (circles), the previous IXS [18] (triangles) and INS [17] (crosses) measurements. A dashed line shows the adiabatic value from the ultrasonic sound measurement [7]. A solid line and a dot–dashed line are guides for the eyes. The M–NM transition temperature is estimated to be around 300–350 °C [25, 26] in the supercooled region.

compressibility β_{HF},[5] and the difference between v_{IXS} and v_s is the excess compressibility itself:

$$v_{IXS} \simeq v_{HF} \equiv \frac{1}{\sqrt{\rho\beta_{HF}}} = \frac{1}{\sqrt{\rho(\beta_S - \beta_r)}}, \qquad v_s = \frac{1}{\sqrt{\rho\beta_S}}. \tag{6}$$

The specific formulation of β_r can be deduced by assuming a simple two-state model (see figure 6)[6]. If the two states are in equilibrium with an energy difference ΔG, an equilibrium constant K can be written as

$$K = \frac{x}{1-x} = \exp\left(-\frac{\Delta G}{k_B T}\right). \tag{7}$$

Thus, the excess compressibility is expressed as

$$\beta_r = \frac{x(1-x)}{k_B T}\left(\frac{|\Delta V|}{V}\right)\left(\frac{\partial \Delta G}{\partial P}\right)_S \tag{8}$$

with ΔV the molar volume difference between the two states. When the energy difference is just the density difference $\Delta G = |-p\Delta V|$, as shown in figure 6(a), the excess compressibility is

$$\beta_r = \frac{x(1-x)}{k_B T}\left(\frac{|\Delta V|}{V}\right)|\Delta V|. \tag{9}$$

[5] For liquid Te, the specific heat ratio is almost 1.0 near the melting temperature and we neglect the difference between the adiabatic and isothermal compressibilities.

[6] We know that the two-state model is too simple to *quantitatively* describe the supercritical state which we suggest in a later part of the present paper, but we think that it is adequate *qualitatively*, and introduce this model for simplicity.

Table 1. β_r estimated from two methods. See the text for details.

Temperature (°C)	500	650	800
x	0.88	0.97	0.99
$\|\Delta V\|/V$	0.15	0.22	0.27
β_r from IXS (TPa^{-1})	103	70	46
β_r from volume (TPa^{-1})	7	4	1

β_r is proportional to the square of the volume inhomogeneity $|\Delta V|$. This is the normal slowing-down phenomenon which is commonly observed in the density fluctuations near the liquid–gas critical point. For ordinary fluids, β_r shows 3D Ising class divergence with the approach to the critical point [28]. But when ΔG has another contribution from the internal energy difference, $\Delta G = |-p\Delta V + \Delta E|$ as shown in figure 6(b), where we suppose that ΔE should be large because the energy difference between metallic and nonmetallic states is expected to be of 10^{-1} eV order while $|-p\Delta V| \sim 10^{-5}$ eV, this becomes

$$\beta_r = \frac{x(1-x)}{k_B T}\left(\frac{|\Delta V|}{V}\right)\left(|\Delta V| + \left(\frac{\partial \Delta E}{\partial P}\right)_S\right). \tag{10}$$

β_r is enhanced by the pressure variation of ΔE.

We apply this formulation to the present result. From equation (6) and the observed positiveness, β_r can be calculated, while β_r is also estimated from equation (9) using the values of x [12] and $|\Delta V|$ [9] from the literature. The results are summarized in table 1. β_r estimated from the pure density inhomogeneity is much smaller than that obtained from the present IXS measurement. Thus, we need to consider other contributions. The enhancement factor $(=|\Delta V| + (\frac{\partial \Delta E}{\partial P})_S \sim (\frac{\partial \Delta E}{\partial P})_S)$ should be very large—more than 10—according to equation (10).

As is shown above, it may be difficult to estimate exact $(\frac{\partial \Delta E}{\partial P})_S$ for liquid Te from the available data. However, the experimental results for another fluid for the M–NM transition would help us to validate the present thermodynamic consideration. In supercritical fluid Hg, the M–NM transition occurs at the density of 9 g cm^{-3} near the liquid–gas critical point [29]. Thus fluctuations are induced by the liquid–gas critical phenomena in the transition region [30]. Ishikawa *et al* [31] carried out IXS measurements on supercritical fluid Hg and reported that the excitation energy of the acoustic mode disperses three times faster than the adiabatic sound velocity at around the M–NM transition. This is crucial information; the enhancement factor is inferred to be very large. Similarly the ultrasonic absorption measurements for supercritical fluid Hg show that the absorption coefficient exhibits double peaks at 9 g cm^{-3} in the M–NM transition and at the critical density (5.8 g cm^{-3}) [32]. Since the absorption coefficient for ultrasonic waves is proportional to β_r [32], these results from the ultrasonic measurements hint that the enhancement factor becomes large at the M–NM transition while the effect of the density fluctuations becomes dominant near the liquid–gas critical region. From the results for liquid Te and fluid Hg, we can speculate that the enhancement factor becomes very large on approaching the M–NM transition region. The large enhancement factor implies that the M–NM transition

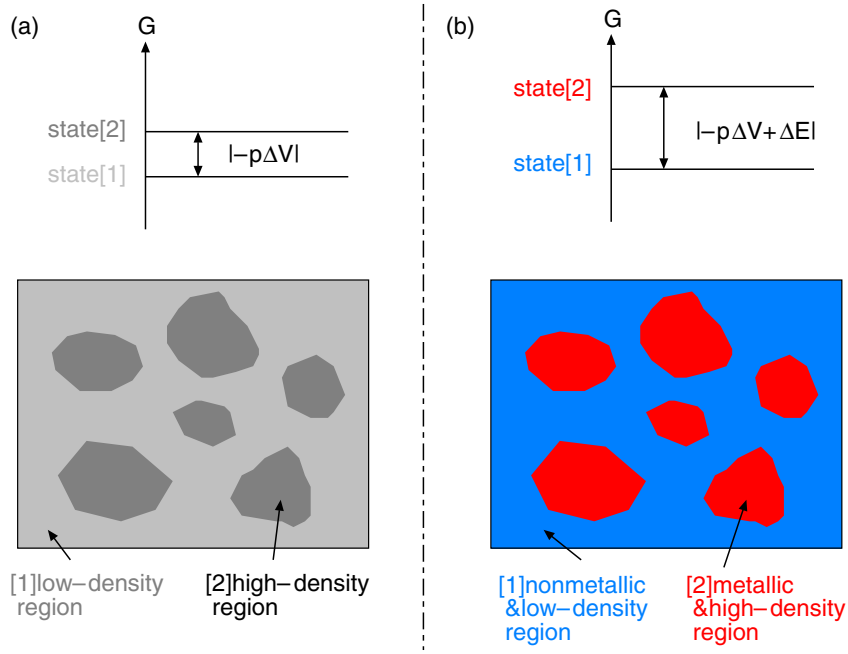

Figure 6. The two-state model and a schematic diagram of the inhomogeneity in the fluid system. (a) Pure density inhomogeneity and (b) density inhomogeneity with metallic nature difference.

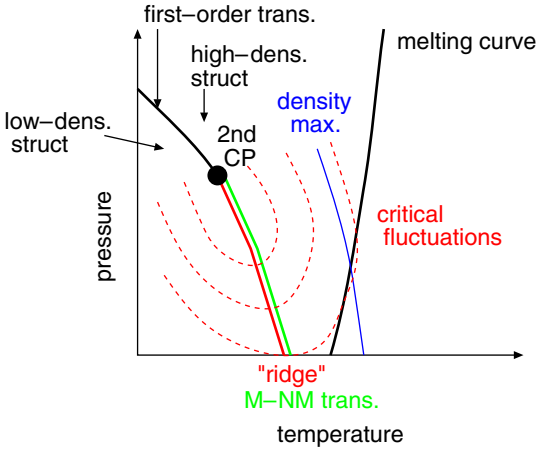

Figure 7. Schematic phase diagram of liquid Te. See the text for details.

is essentially first order in these systems, because ΔE and its derivative with respect to P must show stepwise behavior at the M–NM transition point. We can also conclude that this is the origin of the first problem for liquid Te which is mentioned in the introduction section: there is only a small *density* inhomogeneity but there exists a large *dynamical* inhomogeneity near the melting temperature for liquid Te.

In order to solve the second problem, of why there is inhomogeneity in liquid Te, it may be effective to pay attention to the similarity between liquid Te and water. In a water system, a *second* critical concept has been suggested to explain the complexity of the liquid: in the supercooled region, there exist two liquid states, high density and low density liquids, and the first-order transition between these two phases has a *second* critical point [33, 34] (of course, the first one is the liquid–gas critical point). According to this concept, the structure and thermodynamics of water at ambient conditions are affected by the *second* critical fluctuations. By simply introducing this concept for liquid Te, the second problem can be solved: inhomogeneity of liquid Te is induced by the *second* critical fluctuations, as shown in figure 7, where liquid Te has two phases, which are the metallic high density and nonmetallic low density ones. The first-order transition between these two phases exists in the supercooled region and a second critical point exists. Thus, this phase transition at ambient pressure, which is expected to be under critical pressure, should become second order and will exhibit a continuous change in the supercooled region. In fact, with decreasing temperature, continuous changes were observed in the structure down to 300 °C [25] and the electrical conductivity down to 370 °C [26] for supercooled liquid Te.

5. Conclusion

We have observed the temperature dependence of the dynamical sound velocity of liquid Te by an IXS technique and found that with decreasing temperature, it increases, while the ultrasonic sound velocity decreases. Thus the positiveness exhibits a large value of 70% near the melting temperature, compared to the 10–20% reported for many liquid metals. We introduced a dynamical inhomogeneity, which is defined as the fluctuations with respect to the internal degree of freedom, from the thermodynamic formulation, and explained that when there is a large dynamical inhomogeneity in the system, the positiveness becomes large and the value will be greatly enhanced at the M–NM transition. The present results should be direct evidence of a large dynamical inhomogeneity near the melting temperature in liquid Te, which is observed for the first

time. Next we considered why there appears a large dynamical inhomogeneity for liquid Te. We noticed the similarity of the structural transition in liquid Te and that in liquid water, which reminded us of the idea of second critical fluctuations whose phase diagram has a second critical point. When the second critical fluctuations due to the structural transition which accompanies the M–NM transition are assumed, the large dynamical inhomogeneity near the melting point for liquid Te may be understood naturally.

We concluded that the IXS technique is a powerful tool for investigating the second critical fluctuations when the ultrasonic measurements are combined.

Acknowledgments

This work was supported by Grands-in-Aid for Scientific Research from the Ministry of Education, Culture, Sports, Science and Technology of Japan. The synchrotron radiation experiments were performed at SPring-8 with the approval of the Japan Synchrotron Radiation Research Institute (JASRI; Proposal No. 2005B0093).

References

[1] Epstein A S, Fritzche H and Lark-Horovitz K 1957 *Phys. Rev.* **107** 412
[2] Cabane B and Friedel J 1971 *J. Physique* **32** 73
[3] Tourand G and Breil M 1970 *C. R. Acad. Sci. Paris* B **270** 109
[4] Thurn H and Ruska J 1976 *J. Non-Cryst. Solids* **22** 331
[5] Takeda S, Okazaki H and Tamaki S 1985 *J. Phys. Soc. Japan* **54** 1890
[6] Gitis M B and Mikhailov I G 1966 *Sov. Phys.—Acoust.* **12** 14
[7] Tsuchiya Y 1991 *J. Phys. Soc. Japan* **60** 960
[8] Debenedetti P G 1996 *Metastable Liquids. Concepts and Principles* (Princeton, NJ: Princeton University Press)
[9] Tsuchiya Y and Seymour E F W 1982 *J. Phys. C: Solid State Phys.* **15** L687
Tsuchiya Y and Seymour E F W 1985 *J. Phys. C: Solid State Phys.* **18** 4721
[10] Johnson V A 1955 *Phys. Rev.* **98** 1567
[11] Rapoport E 1968 *J. Chem. Phys.* **48** 1433
[12] Cohen M H and Jortner J 1976 *Phys. Rev.* B **13** 5255
[13] Endo H, Maruyama K, Hoshino H and Ikemoto H 2003 *Z. Phys. Chem.* **217** 863 and references therein
[14] Axmann A, Gissler W, Kollmar A and Springer T 1970 *Discuss. Faraday Soc.* **50** 74
[15] Endo H, Tsuzuki T, Yao M, Kawakita Y, Shibata K, Kamiyama T, Misawa M and Suzuki K 1994 *J. Phys. Soc. Japan* **63** 3200
[16] Chiba A, Ohmasa Y and Yao M 2003 *J. Chem. Phys.* **119** 9047
[17] Ruiz-Martin M D, Jimenez-Ruiz M, Bermejo F J and Fernandez-Perea R 2006 *Phys. Rev.* B **73** 094201
[18] Hosokawa S, Pilgrim W-C, Demmel F and Albergamo F 2006 *J. Non-Cryst. Solids* **352** 5114
[19] Kajihara Y, Inui M, Hosokawa S, Matsuda K and Baron A Q R 2008 *J. Phys.: Conf. Ser.* **98** 022001
[20] Baron A, Tanaka Y, Miwa D, Ishikawa D, Mochizuki T, Takeshita K, Goto S, Matsushita T, Kimura H, Yamamoto F and Ishikawa T 2001 *Nucl. Instrum. Methods* A **467/468** 627
[21] Tamura K, Inui M and Hosokawa S 1999 *Rev. Sci. Instrum.* **70** 144
[22] Hosokawa S and Pilgrim W-C 2001 *Rev. Sci. Instrum.* **72** 1721
[23] Misawa M 1992 *J. Phys.: Condens. Matter* **4** 9491
[24] Barrue R and Perron J C 1985 *Phil. Mag.* B **51** 317
[25] Tsuzuki T, Yao M and Endo H 1995 *J. Phys. Soc. Japan* **64** 485
[26] Perron J C 1967 *Adv. Phys.* **16** 657
[27] Litovitz T A and Davis C M 1965 *Physical Acoustics* vol IIA, ed W P Mason (New York: Academic) chapter 5
Stuehr J and Yeager E 1965 *Physical Acoustics* vol IIA, ed W P Mason (New York: Academic) chapter 6
[28] See e.g., Chaikin P M and Lubensky T C 1995 *Principles of Condensed Matter Physics* (Cambridge: Cambridge University Press) chapter 5.4
[29] Hensel F and Warren W W Jr 1999 *Fluid Metals* (Princeton, NJ: Princeton University Press)
[30] Inui M, Matsuda K, Ishikawa D, Tamura K and Ohishi Y 2007 *Phys. Rev. Lett.* **98** 185504
[31] Ishikawa D, Inui M, Matsuda K, Tamura K, Tsutsui S and Baron A Q R 2004 *Phys. Rev. Lett.* **93** 097801
[32] Kohno H and Yao M 2001 *J. Phys.: Condens. Matter* **13** 10293
[33] See review: Debenedetti P G and Stanley H E 2003 *Phys. Today* **56** 40
[34] Liu L, Chen S H, Faraone A, Yen C W and Mou C Y 2005 *Phys. Rev. Lett.* **95** 117802